crystals

MDPI

Article

Halogen and Hydrogen Bonding in Multicomponent Crystals of Tetrabromo-1*H*-Benzotriazole

Michele Baldrighi, Pierangelo Metrangolo, Tullio Pilati, Giuseppe Resnati * and Giancarlo Terraneo

Laboratory of Nanostructured Fluorinated Materials (NFMLab), Department of Chemistry, Materials, and Chemical Engineering "Giulio Natta", Politecnico di Milano, via L. Mancinelli 7, I-20131 Milano, Italy; michele.baldrighi@polimi.it (M.B.); pierangelo.metrangolo@polimi.it (P.M.); tullio.pilati@gmail.com (T.P.); giancarlo.terraneo@polimi.it (G.T.)

* Correspondence: giuseppe.resnati@polimi.it; Tel.: +39-02-2399-3032

Academic Editor: Peter Politzer

Received: 18 September 2017; Accepted: 26 October 2017; Published: 31 October 2017

Abstract: 4,5,6,7-Tetrabromo-1*H*-benzotriazole (TBBT) is still considered a reference inhibitor of casein kinase II (CK2), a valuable target for anticancer therapy, even though the poor solubility in water of this active pharmaceutical ingredient (API) has prevented its implementation in therapy. We decided to explore the interactions preferentially formed by TBBT in crystalline solids in order to obtain information helpful for the development of new TBBT cocrystals possibly endowed with improved bioavailability. In this paper, we describe the synthesis and the structural characterization of the TBBT methanol solvate and of the TBBT salt with *N*,*N*,*N*′,*N*′-tetramethylethylenediamine. It is shown that TBBT can give rise to several competing interactions. This API is clearly a good halogen bond (XB) donor, with bromine atoms adjacent to the triazole ring possibly better donors than the two others. TBBT is also a good hydrogen bond (HB) donor, with the triazole hydrogen forming an HB with the acceptor or being transferred to it. Interestingly, one of the triazole nitrogens was proven to be able to work as a hydrogen bond acceptor.

Keywords: halogen bonding; hydrogen bonding; supramolecular chemistry; self-assembly; pharmaceutical cocrystals; solvates

1. Introduction

Casein kinase II (CK2) is an enzyme involved in DNA repair, hence it is considered a target for the development of anticancer drugs [1–8]. A CK2 inhibitor recently entered Phase II clinical trials to obtain approval as an anticancer drug for human use [9,10].

4,5,6,7-Tetrabromo-1*H*-benzotriazole (TBBT, Scheme 1) is a small polyhalogenated heterocycle discovered almost 20 years ago. It remains nowadays a particularly potent and selective CK2 inhibitor [1,2,5,7] and is still considered the reference compound among CK2 inhibitors. However, this active pharmaceutical ingredient (API) encountered bioavailability issues that precluded its implementation in anticancer therapy. The four bromine atoms decorating the benzotriazole scaffold are responsible for both the high affinity of the compound for CK2 and its very low solubility in aqueous media [11]. Over the years, several analogues of TBBT have been studied with the aim of improving the potency, selectivity, and solubility in water of this API. Unfortunately, only small improvements have been obtained, despite considerable synthetic efforts to prepare and test libraries of TBBT analogues [6,7,11,12]. The study of analogues of a therapeutically relevant drug is not the only viable strategy when an improved drug solubility and dissolution kinetics are pursued. The synthesis of noncovalent adducts between an API and a suitable cocrystal former (CCF) has been demonstrated to be a fruitful alternative approach. This approach benefits from the fact that the pharmacological

activity of the API remains unaltered in noncovalent adducts, as the molecular structure of the API is unchanged on self-assembly with the CCF and on supramolecular adduct formation [13–16].

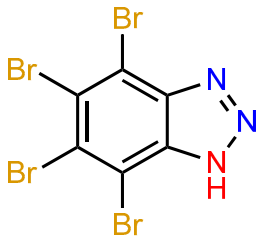

Scheme 1. Molecular structure of 4,5,6,7-tetrabromo-1*H*-benzotriazole (TBBT). Brown: halogen bond (XB) donor sites; red: hydrogen bond (HB) donor site; blue: HB/XB acceptor sites.

When an API–CCF adduct is formed, the recognition and binding phenomena typically occur between molecules displaying a wealth of different functional moieties, which may compete with each other in the formation of the interactions [17–20]. The evaluation of the specific role of the moieties characterized by a similar supramolecular behavior is thus fundamental to identify the most reliable supramolecular synthetic strategies.

Halogen bonding (XB) is the noncovalent interaction wherein a halogen atom, typically bonded to an organic residue, functions as an acceptor of electron density and forms attractive, directional, and short contacts with neutral and anionic electron density donors [21–25]. A large fraction of drugs, both used in clinics and under pre-clinical studies, are halogenated. The specific role of halogen atoms in pinning a drug at the active site of the target enzyme via XB has been proven. In general, the role of XB in affecting binding and recognition phenomena between halogenated residues and biomacromolecules is attracting growing interest [26–28]. In this context, we have recently shown that the formation of halogen-bonded API–CCF cocrystals is a further opportunity offered by this interaction in biopharmacology [29,30]. The relevance of this opportunity is confirmed by the numerous halogen-bonded cocrystals of pharmaceutical interest reported after our papers [31–36].

Thanks to its heavy halogenation, TBBT represents a promising candidate for the synthesis of halogen-bonded pharmaceutical cocrystals. However, this molecule is also a very challenging substrate. The high melting point of pure TBBT (264–266 °C) and its poor solubility in water, as in most organic solvents, suggest the presence of very strong intermolecular API–API interactions in the pure solid compound. Though the crystal structure of the TBBT:CK2 complex has been determined [1], clear indications of the interactions preferentially formed by this API are not available. The TBBT molecular structure displays various electrophilic sites (namely the triazole acidic proton, hydrogen bond (HB) donor, and the aromatic bromine atoms, XB donors), as well as nucleophilic sites (namely the two non-protonated nitrogen atoms of the triazole ring and the benzene π electrons). Consequently, when pursuing the self-assembly of TBBT with a CCF containing basic moieties as XB acceptor sites, the formation of halogen-bonded cocrystals might be hampered by a competition between the basic sites of the CCF and those of TBBT. Alternatively, the XB acceptor sites of the CCF might behave as HB acceptor sites and hydrogen-bonded cocrystal might be formed on interaction of the CCF with the triazole acidic proton.

In this paper, we describe the synthesis and the structural characterization of the TBBT methanol solvate **1** and the TBBT cocrystal with *N*,*N*,*N*′,*N*′-tetramethylethylenediamine (TMEDA) **2**. Information is obtained on the interplay between HB and XB in these two noncovalent adducts, namely on the preferred supramolecular interaction modes of TBBT. This may help in identifying new CCFs generating TBBT pharmaceutical cocrystals with solubility higher than the original API.

2. Results and Discussion

Literature provides few examples of crystal structures where TBBT interacts with proteins, including CK2 [1,37]. In these structures, TBBT is involved in multiple interactions with the protein, namely several XBs between the API bromine atoms and carbonyl oxygens of the protein's backbone, and an HB between the API acidic proton and crystallized water molecules. Although these data provide useful information regarding TBBT's favored supramolecular synthons, their formation may be biased (within certain limits) by the compositional and conformational features of the protein's binding site.

Aiming to obtain the crystal structure of pure TBBT—which has not been reported so far—we undertook a crystallization screening using several solvents and the slow evaporation crystal growth technique. The low solubility of TBBT in water as well as in most of the organic solvents limited the choice of the crystallization conditions, and crystalline samples suitable for single crystal X-ray diffraction studies were obtained only when methanol was used as solvent. Interestingly, the obtained crystals were a TBBT/methanol solvate (**1**). This solvate crystallized in the monoclinic $P2_1/c$ space group and contained TBBT and methanol in a 1:1 ratio. The melting point of this new crystal form is 130 °C, remarkably lower than pure TBBT (264–266 °C). This difference indicates that interactions of TBBT with methanol remarkably modify the pattern of interactions occurring in the pure API.

The crystal structure of **1** shows that the two components of this solvate play a multifaceted role in the crystal packing. Both methanol and TBBT have the dual role of HB donors and acceptors, and TBBT also works as self-complementary XB donor and acceptor (Figure 1). Specifically, short C−Br4···N2 contacts (291.4(4) pm) form halogen-bonded infinite chains, which develop along the *b* crystallographic axis. These XBs are probably rather strong, since the observed Br···N separation corresponds to a normalized contact (Nc) of 0.86 [38], a quite low value for this type of XBs [25]. Consistent with the involvement of the lone pair of N2 in the Br···N XB formation, the bromine atom is nearly coplanar with the triazole ring (the distance of bromine from the mean square plane through the triazole heavy atoms is 15.1 pm) and N1–N2···Br4 and N3–N2···Br4 angles are 115.54° and 135.38°, respectively. Any two adjacent TBBT molecules are further connected by a methanol molecule, which bridges N1 of one molecule and N3 of the other. The former interaction, where TBBT is the HB donor, is much shorter than the latter, where TBBT is the HB acceptor (N···O separations are 277.3(5) and 294.5(5) pm, respectively). This difference is probably related to the fact that TBBT is a weak acid (p*K*a ≈ 5) and a very weak base [5]. These HBs are nearly coplanar with the benzotriazole moiety and, along with the XBs, give rise to nearly planar ribbons that loosely interact with each other [39].

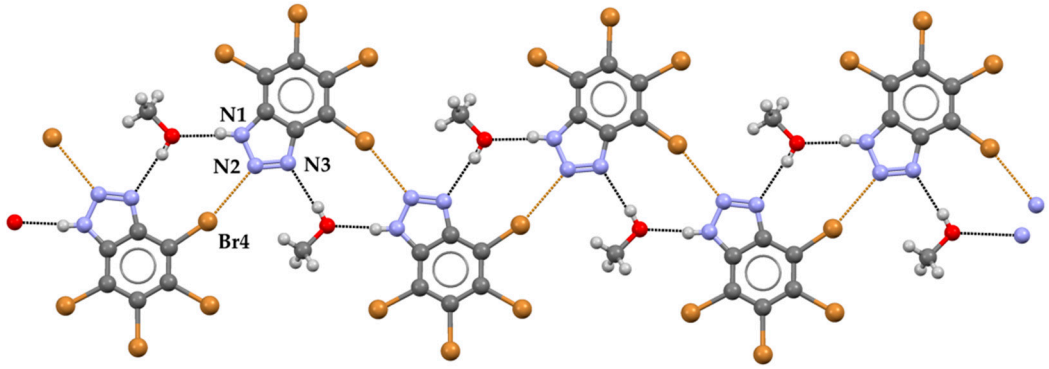

Figure 1. Partial view (Mercury 3.9, ball and stick representation) of one ribbon in the crystal structure of **1**. XBs and HBs are brown and black dotted lines, respectively. Color code: carbon, grey; hydrogen, light grey; nitrogen, light blue; bromine, brown; oxygen, red.

The interaction pattern observed in solvate **1** suggests that TBBT is a good XB and HB donor. Thus, we decided to gain further insights in the TBBT interaction modes by probing it with a stronger XB and

HB acceptor, namely *N*,*N*,*N*′,*N*′-tetramethylethylenediamine (TMEDA). Slow isothermal evaporation of a TBBT and TMEDA solution (2:1 molar ratio) in isopropanol afforded crystals **2**, which melt at 190 °C, also in this case at a lower temperature than pure TBBT. Single crystal X-ray analysis indicates that the system crystallizes in the monoclinic $P2_1/c$ space group and that the two components are present in a 2:1 ratio, as in the starting solution. In the cocrystal, TBBT and TMEDA are involved in a net of XB and HB contacts. Consistent with the Δp*K*a of the involved species [40], the occurrence of a proton transfer from TBBT to TMEDA is preferred over the formation of an HB. In the formed salt, a fairly short HB exist between the N–H4 groups of bis-protonated TMEDA and N1 of the benzotriazole anions (N···N distance is 269.4(3) pm). These HBs give rise to well-defined trimeric units (Figure 2).

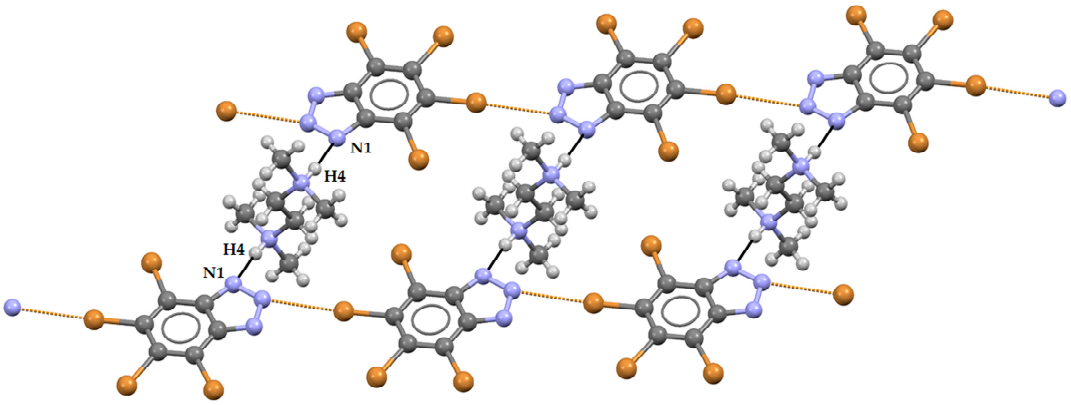

Figure 2. Three bis-protonated TMEDA molecules and hydrogen-bonded TBBT units (Mercury 3.9, ball and stick representation). HBs are represented by black lines; Br···N halogen bonds are represented by brown dotted lines. The color code of atoms is the same as that in Figure 1.

As in solvate **1**, TBBT in **2** acts as a self-complementary module and forms halogen-bonded infinite chains along the crystallographic *a* axis (Figure 3). Br3 atoms act as XB donors, N2 atoms act as XB acceptors and the separation of the formed Br3···N2 XB is 307.1(3) pm (Nc = 0.90). The C−Br3···N2 angle is 172.31(9)°, namely the interaction is close to linearity, a distinctive feature of strong XBs. These halogen-bonded chains are connected to each other by Br···π XBs, where the Br1 atoms of one chain are the XB donors, while the benzene rings π electrons of an adjacent chain work as XB acceptors. Specifically, Br1 atom points almost perpendicular towards the midpoint of C4–C5 bond, with Br1···C4 and Br1···C5 distances of 331.5 and 331.8 pm (Nc = 0.93 for both contacts) and Br3–C4···Br1 and Br4–C5···Br1 angles of 97.79° and 98.89°, respectively.

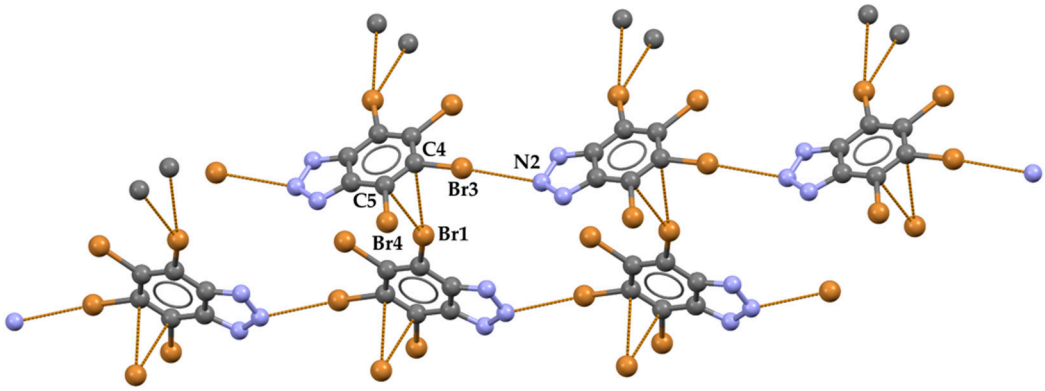

Figure 3. Partial view (Mercury 3.9) of two infinite chains formed by Br···N halogen bonds and bridged by Br···π halogen bonds. Both halogen bond types are brown dotted lines. The color code of atoms is the same as that in Figure 1.

Both Br···N and Br···π XBs are short and occur with the geometries close to the theoretical ones. These features are typical for strong XBs [25]. The likely strength of these XBs and their importance in determining the crystal packing is corroborated by the fact that TBBT molecules interacting via Br···π XBs, and the respective chains, are orthogonal to each other. This configuration has quite demanding steric requirements and is enacted by the network of XBs despite the overall crystal packing of **2** is largely determined by the strong cations/anions electrostatic attraction.

3. Materials and Methods

Starting materials, solvents, and reagents were purchased from Sigma-Aldrich (Merck KGaA, Darmstadt, Germany) in high purity grade and used without further purification. NMR spectra were collected on a Bruker AV400 spectrometer (Bruker BioSpin GmbH, Rheinstetten, Germany). FTIR spectra were collected using a Nicolet Nexus FTIR spectrometer (Thermo Fisher Scientific Inc., Waltham, MA, USA) equipped with Smart Endurance Attenuated Total Reflectance (ATR) device, and analyzed using Nicolet's Omnic®software (Thermo Fisher Scientific Inc., Waltham, MA, USA). Peak values are given in wavenumbers (cm^{-1}) upon automatic assignment. Melting points were collected using a Linkam Hot-Stage microscopy apparatus (Linkam Scientific Instruments, Tadworth, UK). Multicomponent crystals were obtained by slow evaporation from solutions in the appropriate solvent. Crystals were separated from the mother solutions before complete evaporation of the solvent occurred and crystals suitable for X-ray crystallography were selected using an optical microscope. X-ray diffraction data were collected on a Bruker-KAPPA-APEX II CCD diffractometer (Bruker AXS GmbH, Karlsruhe, Germany) using Mo Kα radiation (λ = 0.71073 Å). Data integration and reduction were performed using SaintPlus 6.01 (Bruker, Madison, WI, USA). Absorption correction was performed with a multi-scan method implemented in SADABS (University of Gottingen, Gottingen, Germany) [41,42]. Structures were solved using SHELXS-97 (direct methods) and refined using SHELXL-97 (University of Gottingen, Gottingen, Germany) [43] (full-matrix least-squares on F^2) contained in APEX II and WinGX v1.80.01 software packages [44]. All non-hydrogen atoms were refined anisotropically. Hydrogen atom solution and treatment: In **1**, the O–H hydrogen atom on methanol and H1–N1 were found from a difference map, while other H atoms were placed in geometrically calculated positions and included in the refinement process using a riding model with isotropic thermal parameters. The O–H hydrogen atom on the methanol was refined with soft restraints, and the H1–N1 distance was refined without restraints. In **2**, the hydrogen atom H4 was found from the difference map and refined isotropically without restraints, while all the other H atoms were placed in geometrically calculated positions and included in the refinement process using a riding model with isotropic thermal parameters. Crystallographic data for **1** and **2** are reported in Table S1. CCDC 1574367 and 1574368 contain the supplementary crystallographic data for this paper. The data can be obtained free of charge from The Cambridge Crystallographic Data Centre via www.ccdc.cam.ac.uk/structures. Analysis of crystal data was performed with Mercury 3.9.

Synthesis of 4,5,6,7-tetrabtomobenzotriazole (TBBT): TBBT was synthesized based on literature procedures [45]. Five hundred milligrams of 1*H*-benzotriazole (4.19 mmol), concentrated nitric acid (6.3 mL), and 3.02 g of bromine (18.8 mmol) were placed in a round bottom flask equipped with a magnetic stirrer. The reaction was stirred at reflux (120 °C) for 3 days, the product precipitating from the reaction in the form of a yellow powder. The powder was then recovered by filtration and recrystallized twice from hot acetic acid, giving TBBT as pale yellow crystalline powders (950 mg, 51% yield). m.p.: 262–264 °C; ^{13}C NMR (101 MHz, CD_3OD) δ (ppm) 149.55, 134.95, 121.46; (ATR)FTIR (ν, selected bands): 3505, 3073, 1627, 1423, 1262, 1175, 773 cm^{-1}.

Synthesis of solvate (**1**)*:* In a glass borosilicate vial, 5 mg (0.012 mmol) of TBBT were dissolved in about 2 mL of hot methanol. Once the solution cooled down, it was allowed to slow evaporate at room temperature under a hood. After 1 day, small clear crystals of a bipyramidal shape were found on the bottom of the vial. m.p.: 130–131 °C; (ATR)FTIR (ν, selected bands): 2956, 2871, 1725, 1471, 1262, 1177, 1010, and 863 cm^{-1}.

Synthesis of salt (**2**): Fourteen milligrams of *N*,*N*,*N*′,*N*′-tetramethylethylenediamine (0.13 mmol) were added neat to a solution of 55 mg of TBBT (0.013 mmol) in isopropanol (about 20 mL) in a borosilicate glass vial. The solution was allowed to evaporate slowly under a hood. After 4 days, small yellowish crystalline blocks were found on the bottom of the vial. m.p.: 190–192 °C; (ATR)FTIR (υ, selected bands): 2088, 1397, 1377, 1157, 1088, 761, 699 cm^{-1}.

4. Conclusions

The crystal structure determination of the solvate (**1**) and the salt (**2**) of TBBT confirms indications from the TBBT:CK2 complex [1] that the pattern of interaction preferentially formed by this API is not dominated by a single interaction but is the synergistic result of the balanced contribution of several different attractive forces. The crystal structures of **1** and **2** show that bromine atoms adjacent to the triazole ring (Br1 and Br4) are preferentially involved in XB formation. The same occurs when TBBT forms a complex with CK2 and CDK2 [1,37], and it might thus be suggested that Br1 and Br4 are better XB donors than Br2 and Br3.

In the structures of both **1** and **2**, TBBT forms halogen-bonded chains by acting as a self-complementary module. Self-complementarity between XB donor (Br atoms) and acceptor sites (N2 or π electrons) might drive intermolecular recognition phenomena in pure TBBT as well, and these interactions might be responsible for the poor solubility of the API and its high melting point. TBBT's tendency to self-associate makes identifying effective CCFs more difficult. Furthermore, several Br atoms in TBBT have a Lewis acid character, allowing for a complex multimodal XB donor behavior of TBBT.

HBs in **1** and **2** involve both the API and the CCF. This suggests that the HB donor site of TBBT (namely the acidic N–H group) may have a general tendency to interact with a variety of molecular partners. It is also interesting that, in the structure of the solvate (**1**), N3 acts as an HB acceptor. To the best of our knowledge, this feature has not been previously observed in any of the reported structures of TBBT:protein assemblies, and suggests that also HB donors might find application as CCFs for the synthesis of TBBT's pharmaceutical cocrystals.

In conclusion, the obtainment of the solvate (**1**) and the salt (**2**) of TBBT, and the structural analyses of the two systems, allowed us to identify interactions consistently formed by this API in crystalline solids. This information might be helpful in further studies where crystal engineering is used to design and synthesize new TBBT cocrystals with improved bioavailability. The obtainment of TBBT's pharmaceutical cocrystals using inorganic anions as XB acceptors are under study to assess if the resulting synthon can displace the C–Br···N2 synthon observed herein.

Supplementary Materials: The following are available online at www.mdpi.com/2073-4352/7/11/332/s1, Figure S1: FTIR spectra of pure TBBT (top) and of the solids obtained on recrystallization of TBBT from methanol, ethanol, trifluoroethanol, *i*-propanol, and acetonitrile (from second to sixth spectrum in the order). Only in the case of methanol were crystals suitable for single crystal X-ray analyses obtained. It seems that pure TBBT was obtained in all cases, except that of ethanol, which might have formed a solvate, or a polymorph, of TBBT. Table S1: Crystallographic data for **1** and **2**.

Acknowledgments: Fondazione Cariplo (grant number 2010-1351) and MIUR (project PRIN 2010–2011, grant number 2010ERFKXL_005) are acknowledged for partial financial support.

Author Contributions: The manuscript was written through contributions of all authors. All authors have given approval to the final version of the manuscript. Michele Baldrighi performed the experiments and wrote the paper; Pierangelo Metrangolo conceived and designed the experiments; Giuseppe Resnati conceived and designed the experiments and wrote the paper; Tullio Pilati and Giancarlo Terraneo collected X-ray data, and solved and refined the reported structures.

Conflicts of Interest: The authors declare no conflicts of interest.

References and Notes

1. Battistutta, R.; De Moliner, E.; Sarno, S.; Zanotti, G.; Pinna, L.A. Structural features underlying selective inhibition of protein kinase CK2 by ATP site-directed tetrabromo-2-benzotriazole. *Protein Sci.* **2001**, *10*, 2200–2206. [CrossRef] [PubMed]

2. Sarno, S.; Reddy, H.; Meggio, F.; Ruzzene, M.; Davies, S.P.; Donella-Deana, A.; Shugar, D.; Pinna, L.A. Selectivity of 4,5,6,7-tetrabromobenzotriazole, an ATP site-directed inhibitor of protein kinase CK2 ('casein kinase-2'). *FEBS Lett.* **2001**, *496*, 44–48. [CrossRef]
3. Zień, P.; Bretner, M.; Zastapiło, K.; Szyszka, R.; Shugar, D. Selectivity of 4,5,6,7-tetrabromobenzimidazole as an ATP-competitive potent inhibitor of protein kinase CK2 from various sources. *Biochem. Biophys. Res. Commun.* **2003**, *306*, 129–133. [CrossRef]
4. Sarno, S.; Moro, S.; Meggio, F.; Zagotto, G.; Dal Ben, D.; Ghisellini, P.; Battistutta, R.; Zanotti, G.; Pinna, L.A. Toward the rational design of protein kinase casein kinase-2 inhibitors. *Pharmacol. Ther.* **2002**, *93*, 159–168. [CrossRef]
5. Zien, P.; Duncan, J.S.; Skierski, J.; Bretner, M.; Litchfield, D.W.; Shugar, D. Tetrabromobenzotriazole (TBBt) and tetrabromobenzimidazole (TBBz) as selective inhibitors of protein kinase CK2: Evaluation of their effects on cells and different molecular forms of human CK2. *Biochim. Biophys. Acta* **2005**, *1754*, 271–280. [CrossRef] [PubMed]
6. Bretner, M.; Najda-Bernatowicz, A.; Łebska, M.; Muszyńska, G.; Kilanowicz, A.; Sapota, A. New inhibitors of protein kinase CK2, analogues of benzimidazole and benzotriazole. *Mol. Cell. Biochem.* **2008**, *316*, 87–89. [CrossRef] [PubMed]
7. Pagano, M.A.; Bain, J.; Kazimierczuk, Z.; Sarno, S.; Ruzzene, M.; Di Maira, G.; Elliott, M.; Orzeszko, A.; Cozza, G.; Meggio, F.; et al. The selectivity of inhibitors of protein kinase CK2: An update. *Biochem. J.* **2008**, *415*, 353–365. [CrossRef] [PubMed]
8. Unger, G.M.; Davis, A.T.; Slaton, J.W.; Ahmed, K. Protein kinase CK2 as regulator of cell survival: Implications for cancer therapy. *Curr. Cancer Drug Targets* **2004**, *4*, 77–84. [CrossRef] [PubMed]
9. Siddiqui-Jain, A.; Drygin, D.; Streiner, N.; Chua, P.; Pierre, F.; O'Brien, S.E.; Bliesath, J.; Omori, M.; Huser, N.; Ho, C.; et al. CX-4945, an orally bioavailable selective inhibitor of protein kinase CK2, inhibits prosurvival and angiogenic signaling and exhibits antitumor efficacy. *Cancer Res.* **2010**, *70*, 10288–10298. [CrossRef] [PubMed]
10. Martins, L.R.; Lúcio, P.; Melão, A.; Antunes, I.; Cardoso, B.A.; Stansfield, R.; Bertilaccio, M.T.S.; Ghia, P.; Drygin, D.; Silva, M.G.; et al. Activity of the clinical-stage CK2-specific inhibitor CX-4945 against chronic lymphocytic leukemia. *Leukemia* **2014**, *28*, 179–182. [CrossRef] [PubMed]
11. Wasik, R.; Wińska, P.; Poznański, J.; Shugar, D. Synthesis and physico-chemical properties in aqueous medium of all possible isomeric bromo analogues of benzo-1*H*-triazole, potential inhibitors of protein kinases. *J. Phys. Chem. B* **2012**, *116*, 7259–7268. [CrossRef] [PubMed]
12. Gianoncelli, A.; Cozza, G.; Orzeszko, A.; Meggio, F.; Kazimierczuk, Z.; Pinna, L.A. Tetraiodobenzimidazoles are potent inhibitors of protein kinase CK2. *Bioorg. Med. Chem.* **2009**, *17*, 7281–7289. [CrossRef] [PubMed]
13. Shan, N.; Zaworotko, M.J. The role of cocrystals in pharmaceutical science. *Drug Discov. Today* **2008**, *13*, 440–446. [CrossRef] [PubMed]
14. Kawakami, K. Modification of physicochemical characteristics of active pharmaceutical ingredients and application of supersaturatable dosage forms for improving bioavailability of poorly absorbed drugs. *Adv. Drug Deliv. Rev.* **2012**, *64*, 480–495. [CrossRef] [PubMed]
15. Elder, D.P.; Holm, R.; De Diego, H.L. Use of pharmaceutical salts and cocrystals to address the issue of poor solubility. *Int. J. Pharm.* **2013**, *453*, 88–100. [CrossRef] [PubMed]
16. Babu, N.J.; Nangia, A. Solubility advantage of amorphous drugs and pharmaceutical cocrystals. *Cryst. Growth Des.* **2011**, *11*, 2662–2679. [CrossRef]
17. Anderson, K.M.; Goeta, A.E.; Steed, J.W. Supramolecular Synthon Frustration Leads to Crystal Structures with $Z' > 1$. *Cryst. Growth Des.* **2008**, *8*, 2517–2524. [CrossRef]
18. Babu, N.J.; Cherukuvada, S.; Thakuria, R.; Nangia, A. Conformational and Synthon Polymorphism in Furosemide (Lasix). *Cryst. Growth Des.* **2010**, *10*, 1979–1989. [CrossRef]
19. Aakeröy, C.B.; Wijethunga, T.K.; Haj, M.A.; Desper, J.; Moore, C. The structural landscape of heteroaryl-2-imidazoles: Competing halogen- and hydrogen-bond interactions. *CrystEngComm* **2014**, *16*, 7218. [CrossRef]
20. Aakeröy, C.B.; Panikkattu, S.; Chopade, P.D.; Desper, J. Competing hydrogen-bond and halogen-bond donors in crystal engineering. *CrystEngComm* **2013**, *15*, 3125–3136. [CrossRef]
21. Desiraju, G.R.; Ho, P.S.; Kloo, L.; Legon, A.C.; Marquardt, R.; Metrangolo, P.; Politzer, P.; Resnati, G.; Rissanen, K. Definition of the halogen bond (IUPAC Recommendations 2013). *Pure Appl. Chem.* **2013**, *85*, 1711–1713. [CrossRef]

22. Metrangolo, P.; Neukirch, H.; Pilati, T.; Resnati, G. Halogen bonding based recognition processes: A world parallel to hydrogen bonding. *Acc. Chem. Res.* **2005**, *38*, 386–395. [CrossRef] [PubMed]
23. Beale, T.M.; Chudzinski, M.G.; Sarwar, M.G.; Taylor, M.S. Halogen bonding in solution: Thermodynamics and applications. *Chem. Soc. Rev.* **2013**, *42*, 1667–1680. [CrossRef] [PubMed]
24. Politzer, P.; Murray, J.S.; Clark, T. Halogen bonding: An electrostatically-driven highly directional noncovalent interaction. *Phys. Chem. Chem. Phys.* **2010**, *12*, 7748–7757. [CrossRef] [PubMed]
25. Cavallo, G.; Metrangolo, P.; Milani, R.; Pilati, T.; Priimagi, A.; Resnati, G.; Terraneo, G. The halogen bond. *Chem. Rev.* **2016**, *116*, 2478–2601. [CrossRef] [PubMed]
26. Parisini, E.; Metrangolo, P.; Pilati, T.; Resnati, G.; Terraneo, G. Halogen bonding in halocarbon-protein complexes: A structural survey. *Chem. Soc. Rev.* **2011**, *40*, 2267–2278. [CrossRef] [PubMed]
27. Auffinger, P.; Hays, F.A.; Westhof, E.; Ho, P.S. Halogen bonds in biological molecules. *Proc. Natl. Acad. Sci. USA* **2004**, *101*, 16789–16794. [CrossRef] [PubMed]
28. Voth, A.R.; Hays, F.A.; Ho, P.S. Directing macromolecular conformation through halogen bonds. *Proc. Natl. Acad. Sci. USA* **2007**, *104*, 6188–6193. [CrossRef] [PubMed]
29. Baldrighi, M.; Bartesaghi, D.; Cavallo, G.; Chierotti, M.R.; Gobetto, R.; Metrangolo, P.; Pilati, T.; Resnati, G.; Terraneo, G. Polymorphs and co-crystals of haloprogin: an antifungal agent. *CrystEngComm* **2014**, *16*, 5897–5904. [CrossRef]
30. Baldrighi, M.; Cavallo, G.; Chierotti, M.R.; Gobetto, R.; Metrangolo, P.; Pilati, T.; Resnati, G.; Terraneo, G. Halogen bonding and pharmaceutical cocrystals: The case of a widely used preservative. *Mol. Pharm.* **2013**, *10*, 1760–1772. [CrossRef] [PubMed]
31. Aakeröy, C.B.; Welideniya, D.; Desper, J.; Moore, C. Halogen-bond driven co-crystallization of potential anti-cancer compounds: A structural study. *CrystEngComm* **2014**, *16*, 10203–10209. [CrossRef]
32. Miroslaw, B.; Plech, T.; Wujec, M. Halogen bonding in the antibacterial 1,2,4-triazole-3-thione derivative—Spectroscopic properties, crystal structure and conformational analysis. *J. Mol. Struct.* **2015**, *1083*, 187–193. [CrossRef]
33. Fucke, K.; McIntyre, G.J.; Lemée-Cailleau, M.H.; Wilkinson, C.; Edwards, A.J.; Howard, J.A.K.; Steed, J.W. Insights into the Crystallisation Process from Anhydrous, Hydrated and Solvated Crystal Forms of Diatrizoic Acid. *Chem. A Eur. J.* **2015**, *21*, 1036–1047. [CrossRef] [PubMed]
34. Valkonen, A.; Chukhlieb, M.; Moilanen, J.; Tuononen, H.M.; Rissanen, K. Halogen and hydrogen bonded complexes of 5-iodouracil. *Cryst. Growth Des.* **2013**, *13*, 4769–4775. [CrossRef]
35. Gerhardt, V.; Egert, E. Cocrystals of 6-chlorouracil and 6-chloro-3-methyluracil: Exploring their hydrogen-bond-based synthon motifs with several triazine and pyrimidine derivatives. *Acta Crystallogr. Sect. B Struct. Sci. Cryst. Eng. Mater.* **2015**, *71*, 209–220. [CrossRef] [PubMed]
36. Golob, S.; Perry, M.; Lusi, M.; Chierotti, M.R.; Grabnar, I.; Lassiani, L.; Voinovich, D.; Zaworotko, M.J. Improving Biopharmaceutical Properties of Vinpocetine Through Cocrystallization. *J. Pharm. Sci.* **2016**, *105*, 3626–3633. [CrossRef] [PubMed]
37. De Moliner, E.; Brown, N.R.; Johnson, L.N. Alternative binding modes of an inhibitor to two different kinases. *Eur. J. Biochem.* **2003**, *270*, 3174–3181. [CrossRef] [PubMed]
38. A normalized contact (Nc) is the ratio between the observed separation of interacting atoms and the sum of their respective van der Waals radii; it allows the different interactions lengths to be more meaningfully compared than when absolute separations are used.
39. Rather long type-I bromine-bromine interactions (Br1···Br3 distance is 360.66(8) Å, corresponding to Nc = 0.97; C−Br···Br angles are 126.1(1)° and 126.5(1)°) connect adjacent and coplanar ribbons and form planes which develop along the *b* crystallographic axis. No contacts below van der Waals radii exist between adjacent planes.
40. Childs, S.L.; Stahly, G.P.; Park, A. The salt-cocrystal continuum: The influence of crystal structure on ionization state. *Mol. Pharm.* **2007**, *4*, 323–338. [CrossRef] [PubMed]
41. Sheldrick, G.M. *SADABS, Empirical Absorption Correction Program*; University of Gottingen: Gottingen, Germany, 1997.
42. Blessing, R.H. An empirical correction for absorption anisotropy. *Acta Crystallogr. Sect. A Found. Crystallogr.* **1995**, *51*, 33–38. [CrossRef]
43. Sheldrick, G.M. A short history of SHELX. *Acta Crystallogr. A* **2008**, *64*, 112–122. [CrossRef] [PubMed]

44. Farrugia, L.J. WinGX suite for small-molecule single-crystal crystallography. *J. Appl. Crystallogr.* **1999**, *32*, 837–838. [CrossRef]
45. Wiley, R.H.; Hussung, K.F. Halogenated Benzotriazoles. *J. Am. Chem. Soc.* **1957**, *79*, 4395–4400. [CrossRef]